Design of Pt-Shell Nanoparticles with Alloy Cores for the Oxygen Reduction Reaction

Liang Zhang,[†,‡,§] Ravikumar Iyyamperumal,[†,‡] David F. Yancey,[†,‡] Richard M. Crooks,[†,‡,*] and Graeme Henkelman[†,‡,§,*]

[†]Department of Chemistry and Biochemistry, [‡]Texas Materials Institute, and [§]Institute for Computational and Engineering Sciences, The University of Texas at Austin, 105 E. 24th Street, Stop A5300, Austin, Texas 78712-1224, United States

ABSTRACT We report that the oxygen binding energy of alloy-core@Pt nanoparticles can be linearly tuned by varying the alloy-core composition. Using this tuning mechanism, we are able to predict optimal compositions for different alloy-core@Pt nanoparticles. Subsequent electrochemical measurements of ORR activities of AuPd@Pt dendrimer-encapsulated nanoparticles (DENs) are in a good agreement with the theoretical prediction that the peak of activity is achieved for a 28% Au/72% Pd alloy core supporting a Pt shell. Importantly, these findings represent an unusual case of first-principles theory leading to nearly perfect agreement with experimental results.

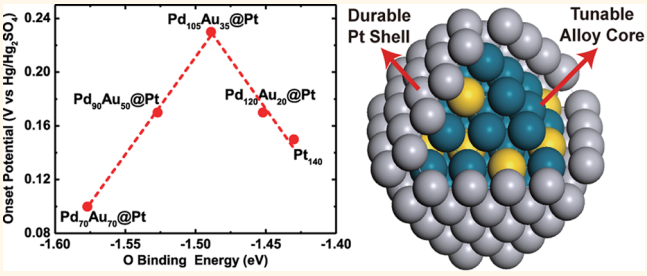

KEYWORDS: oxygen reduction · platinum · core–shell nanoparticles

Catalytic materials containing an atomically thin Pt surface layer are a promising alternative to pure Pt nanoparticle catalysts for the oxygen reduction reaction (ORR). Pt-shelled catalysts can be stable, have significantly less Pt loading than commercial alternatives, and can show higher activities.[1−3] Recent progress has also been made using near-surface alloys to tune the activity of the catalytic surface. One such promising geometry is a monolayer shell covering a random alloy core of variable composition. These alloy-core@shell nanoparticles have both the robustness of core@shell structures and the tunability of random alloy particles.[4] In a recent example, Adzic and co-workers reported that adding Au to a Pd nanoparticle core covered by a Pt monolayer shell enhances stability under ORR conditions.[5,6]

In this study, we predict ORR activity trends of 2 nm alloy-core@Pt-shell nanoparticles using density functional theory (DFT) calculations using oxygen binding as the reactivity descriptor. The combination of Au and Pd in the nanoparticle core is found to be particularly interesting because variations of the core composition between pure Au and pure Pd are calculated to shift the oxygen binding on the Pt shell to values both weaker and stronger than bulk Pt. Our predicted trends in ORR activity, as well as the optimal core composition, provide a testable model for experiments. Accordingly, we show that the measured ORR activities of AuPd@Pt dendrimer-encapsulated nanoparticles (DENs) are in good correlation to our theoretical model, and that a 28% Au/72% Pd alloy-core supports a Pt-shell with activity that is higher than that of monometallic Pt particles.

DENs are well-suited for comparison with theory for the following reasons: (1) they are of a size (<2 nm) where intrinsic nanoscale properties are observed and direct DFT simulations are manageable;[7,8] (2) they can be synthesized in a variety of structural configurations with a degree of atomic level control;[9,10] and (3) the dendrimer surrounding the nanoparticle not only prevents nanoparticle ripening during catalytic reactions but also separates the nanoparticle from the support (electrode), thereby eliminating the need to model support interactions. Crooks and coworkers have shown that different configurations of bimetallic DENs, including random

* Address correspondence to crooks@cm.utexas.edu, henkelman@cm.utexas.edu.

Received for review July 22, 2013 and accepted September 16, 2013.

Published online September 16, 2013
10.1021/nn403788a

alloy and core@shell structures, can be synthesized by various homogeneous methods.[11] They have also used an electrochemical method, originally developed by Adzic and co-workers,[12] to synthesize core@shell DENs *via* underpotential deposition (UPD) and subsequent galvanic exchange.[13,14]

Calculated oxygen (and hydroxyl) binding energies have been demonstrated to be an effective descriptor of ORR activity.[15] A good review of this subject is provided by Mukerjee and Srinivasan, who have summarized the earlier work regarding the correlation between the electrocatalytic activity and the bond strength of the adsorbate for ORR.[16] Using a microkinetic model, including molecular oxygen activation and oxygen species desorption, Nørskov and co-workers have established a volcano-shaped correlation between the oxygen binding energy and ORR activity.[17,18] On the strong-binding branch, the overall activity is limited by the removal of oxygen species, while on the weak-binding branch, oxygen molecule activation limits the reaction. An optimal compromise is found for O binding slightly weaker than that on the bulk Pt(111) surface.[18] In this study, a target O binding energy was chosen, calculated to be −1.51 eV on a five-layer 3 × 3 Pt(111) slab model, using a gas-phase molecular O_2 reference. Although oxygen binding on bulk Pt(111) is not necessarily optimal for ORR, it gives a close enough estimate of the location of the volcano peak to understand trends in nanoparticle activity.

RESULTS AND DISCUSSION

Following our previous work on Pd-shelled particles,[4] the core metals can be classified into two groups: Pd, Cu, Ir, Ru, and Rh reduce the O binding to the Pt shell when they are added into the core, while Au and Ag increase the O binding energy. The target O binding can be achieved by alloying metal X from the first group (X = Pd, Cu, Ir, Rh, and Rh) and metal Y from the second group (Y = Au and Ag) in the core. Figure 1 shows the average O binding energies of (a) X_xAu_{1-x}@Pt and (b) X_xAg_{1-x}@Pt as a function of core composition. The near-linear O binding trends are consistent with our earlier reports for alloy-core@Pd-shell nanoparticles.[4] Optimal alloy-core compositions are predicted at the intersections of linear O binding trends and the target O binding energy (solid and dashed lines in Figure 1, respectively). The predicted optimal alloy-core compositions are listed in Table 1.

The thermodynamic stability of a core−shell structure is also very important if the nanoparticle is to function as a catalyst. Stability can be quantified with calculations of the core/shell segregation energy.[19−21] The segregation energy of Pt-shell NP140 with various monometallic core elements was calculated as the energy required to swap one Pt atom on the (111) facet and its neighboring subsurface core atom. The presence of a surface O adsorbate was also considered to model the oxidizing environment of the ORR. Figure 2 shows the calculated segregation energy of the monometallic-core@Pt-shell nanoparticles with and without bound surface oxygen. Au@Pt, Ag@Pt, Ir@Pt, and Rh@Pt are thermodynamically stable in both vacuum and an oxygen-rich environment. Pd and Ru are expected to be stable as the core of Pt-shell nanoparticles in vacuum. However, the bound oxygen species facilitate the swapping of core and shell atoms under ORR conditions. The Cu@Pt particle is found to be thermodynamically unstable. Notably, although the thermodynamic stability of the Pd@Pt nanoparticle is reduced with surface-bound oxygen species, it has been reported that introducing Au or Ag to the Pd

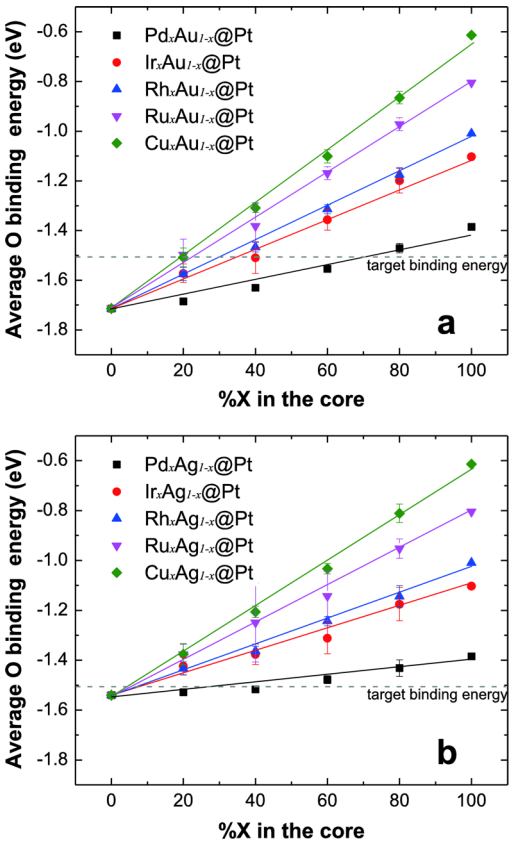

Figure 1. Oxygen binding energy trends for (a) X_xAu_{1-x}@Pt and (b) X_xAg_{1-x}@Pt NP140 (X = Pd, Ir, Rh, Ru, and Cu). The gray dashed line represents the target oxygen binding energy.

TABLE 1. Optimal Ratio of Metal X Alloyed with Au and Ag in the Core of a Pt-Shelled Particle

	metal Y	
metal X	Au	Ag
Pd	0.72	0.30
Ir	0.35	0.09
Rh	0.30	0.08
Ru	0.22	0.07
Cu	0.19	0.05

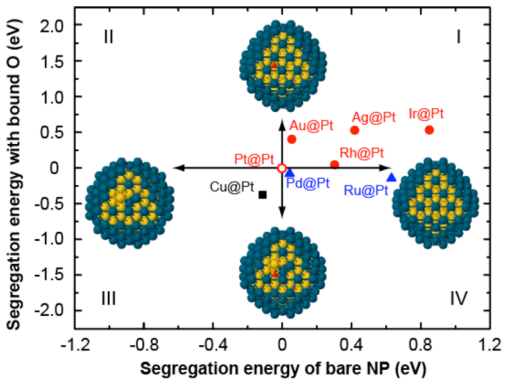

Figure 2. Stability of Pt-shell particles with various core elements. The insets indicate the stable structures along each axial direction.

core can enhance the stability and durability of a Pt surface layer under ORR conditions.[5,22]

Because Au is easier to work with than Ag, we selected PdAu@Pt DENs as our model system for comparison with the foregoing calculations. Briefly, Pd_nAu_{140-n}@Pt DENs were synthesized electrochemically by Cu UPD onto Pd_nAu_{140-n} alloy cores, followed by galvanic exchange of the Cu layer for Pt. The methodology used to prepare these alloy-core@shell DENs is similar to one we have previously reported[8] and is discussed in detail in the Supporting Information. The ORR activity of Au_{140}, Pt_{140}, $Pd_{70}Au_{70}$, and Pd_nAu_{140-n}@Pt (n = 70, 90, 105, and 120) DENs was then determined using rotating disk voltammetry.[10] Note that the subscripts used here reflect the nominal elemental compositions of the DENs based on the percentages of Pd and Au used to prepare them. We have previously shown that these values are good (but not perfect) estimates of the experimentally determined stoichiometry of the nanoparticles.[23,24]

Figure 3a shows a series of rotating disk voltammograms (RDVs) for glassy carbon electrodes modified with Pd_nAu_{140-n}@Pt and Pt_{140} DENs, and Figure 3b shows an expanded portion of these RDVs in the vicinity of the onset of current. The RDVs were obtained in O_2-saturated, aqueous 0.10 M $HClO_4$ using a rotation rate of 1600 rpm at a scan rate of 5 mV/s. The onset potential for the ORR, which is defined as the potential of the inflection point on the quasi-steady-state polarization curve, at the $Pd_{70}Au_{70}$ DEN-modified electrode is −0.30 V. However, upon addition of the Pt shell, this value shifts positive to 0.10 V. For comparison, the ORR onset potential for the Pt_{140} DENs is at 0.15 V, which is more positive than that of the $Pd_{70}Au_{70}$@Pt electrocatalyst. However, the ORR onset potentials for $Pd_{90}Au_{50}$@Pt and $Pd_{120}Au_{20}$@Pt DENs are shifted even more positive, to 0.17 V. The onset potential for the $Pd_{105}Au_{35}$@Pt DENs shifts much more positive, to 0.23 V, than any of the other DENs, and hence it has the lowest overpotential and highest activity. Figure 3c summarizes the RDV data by showing the onset

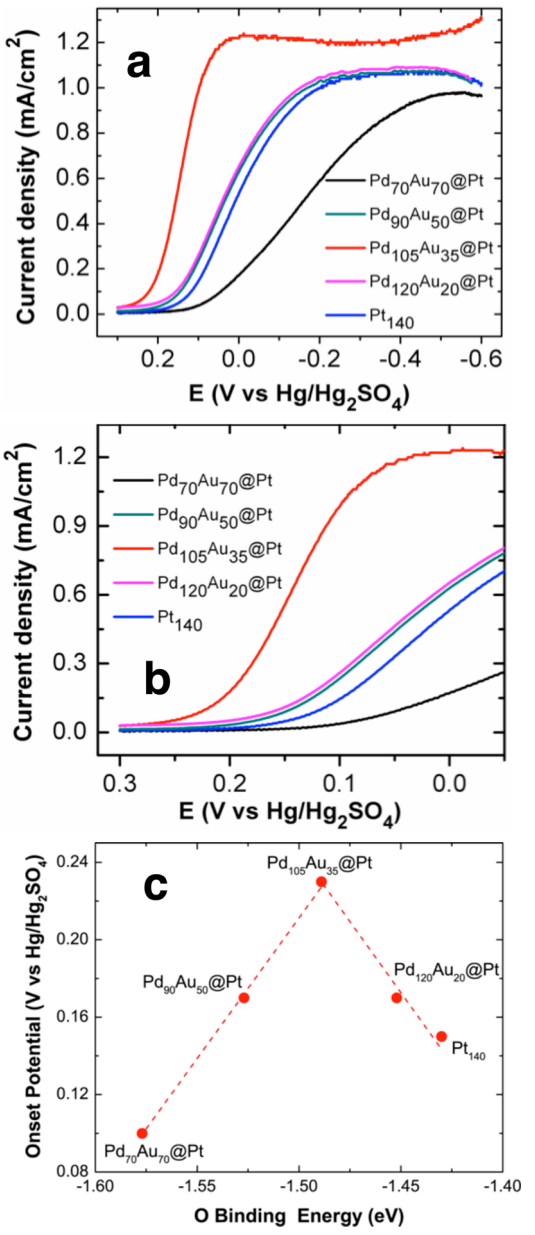

Figure 3. (a) Rotating disk voltammograms for glassy carbon electrodes modified with Pd_nAu_{140-n}@Pt (n = 70, 90, 105, 120) and Pt_{140} DENs. The electrode rotation rate was 1600 rpm, the scan rate was 5 mV/s, the electrolyte solution was O_2-saturated, aqueous 0.10 M $HClO_4$, and the electrode was scanned from −0.6 to 0.3 V (*vs* Hg/Hg_2SO_4). (b) Enlargement of part (a) in the region of the onset potential for the ORR. Note that the current axes in (a) and (b) are normalized to the electrochemical surface area of Pt determined by measuring hydrogen UPD. Full details are provided in Table S1 in the Supporting Information. (c) Onset potential for the ORR at Pd_xAu_{1-x}@Pt DENs measured by RDVs and plotted as a function of the corresponding oxygen binding energy calculated by DFT. The dashed line corresponds to the linear fit of the two branches of the activity volcano.

potential for the ORR as a function of corresponding O binding energy calculated from DFT. The measured activities exhibit a volcano-shaped trend when plotted against the theoretically determined O binding energy. The peak of the volcano, corresponding to $Pd_{105}Au_{35}$@Pt

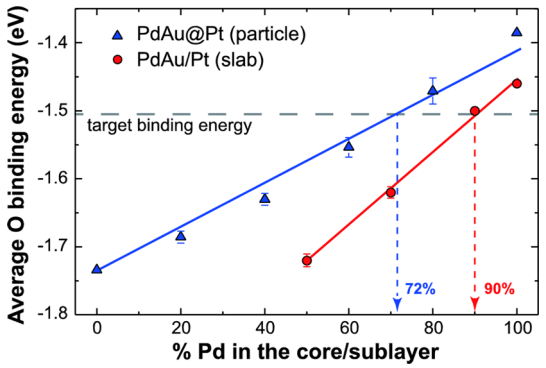

Figure 4. Trends of average oxygen binding energy as a function of core composition for Pd_xAu_{1-x}@Pt (nanoparticle geometry) and PdAu/Pt (slab geometry).

or 75% Pd in the core, is in very good agreement with our theoretical prediction of 72% Pd. Additionally, a Pt shell reduces the Pt loading as compared to a pure Pt particle.

Figure 4 shows the average oxygen binding energy trend of PdAu@Pt NP140 in comparison to a bulk PdAu alloy substrate supporting a monolayer of Pt, denoted as PdAu/Pt. The latter system was chosen to compare with the larger (5.4 nm) PdAu@Pt nanoparticles studied by Adzic and co-workers.[5] Details of these slab calculations can be found in the Supporting Information. Notably, there is a shift in optimal core composition for our ~2 nm DENs (72%) as compared to the slab geometry (90% Pd). The later composition was chosen by the Adzic group for their 5.4 nm nanoparticles. The shift of the activity peak with composition can be explained from two factors: (1) there is weaker O binding to the DENs; and (2) alloying Au to Pd has a more significant effect on the O binding energy to the slab. These factors correspond to the differences in intercepts and slopes of the trend lines in Figure 4, respectively. These two factors can be understood in terms of a strain effect. The shell of Pd@Pt NP140 has an average Pt−Pt bond length of 2.68 Å, which is about 0.07 Å shorter than the surface Pt layer of the Pd/Pt slab. The shorter Pt−Pt bond length causes a higher strain, leading to a weaker oxygen binding energy. On the other hand, the Pt−Pt bond length difference between Pd@Pt and Au@Pt is 0.04 Å, which is smaller than the difference between Pd/Pt and Au/Pt (0.14 Å), resulting in a reduced effect of alloying Au to Pd on the O binding energy.

CONCLUSIONS

In conclusion, we have shown that the oxygen binding energy of alloy-core@Pt-shell nanoparticles can be linearly tuned by varying the composition of the alloy core. An important point pertains to the way this experiment was carried out. First, we obtained the experimental data shown in Figure 3c for just two DEN compositions: $Pd_{70}Au_{70}$@Pt and $Pd_{105}Au_{35}$@Pt. On the basis of these results, we anticipated a simple linear relationship between alloy-core composition and ORR activity. Second, DFT calculations were carried out, and they predicted a volcano-shaped relationship between the onset potential for the ORR, catalyzed by PdAu@Pt NP140 nanoparticles, and the oxygen binding energy. The peak activity was predicted to occur at a core composition corresponding to 105 Pd atoms and 35 Au atoms (Figure 3c). Third, we synthesized and tested additional Pd_nAu_{140-n}@Pt DEN compositions and were gratified to find that the activity of these electrocatalysts fell almost exactly on the predicted trend lines. Hence, this is an unusual case of first-principles theory leading to nearly perfect agreement with experimental results. We believe that this tuning mechanism is a general property of the alloy-core@shell system and hence provides a systematic means for designing nanoparticles to have desirable catalytic activity.

METHOD

Spin-polarized DFT was used to calculate all oxygen binding energies using the Vienna ab initio simulation package.[25,26] Calculation details can be found in the Supporting Information. The nanoparticles were modeled as face-centered cubic (fcc) crystallites in the shape of a 140 atom truncated octahedron (NP140) with 44 core atoms and 96 shell atoms. The alloy core@Pt shell is denoted as X_xY_{1-x}@Pt, where X and Y are the two metals constituting the core, which are chosen from Au, Ag, Pd, Cu, Ir, Ru, and Rh. The fraction of metal X in the alloy core is designated as x. The O binding energy, E_b, was calculated by averaging over the hollow binding sites in the center of each of the eight (111) facets, using eq 1

$$E_b = \frac{1}{8}(E_{NP+8O} - E_{NP} - 4E_{O_2}) \quad (1)$$

where E_{NP+8O} is the energy of the particle with eight oxygen atoms adsorbed, E_{NP} is the energy of the bare particle, and E_{O_2} is the energy of the O_2 molecule chosen as the oxygen reference. Ten different random alloy configurations were generated to calculate the average O binding energy for each core composition (80 binding sites, total).

Conflict of Interest: The authors declare no competing financial interest.

Acknowledgment. We gratefully acknowledge support from the Chemical Sciences, Geosciences, and Biosciences Division, Office of Basic Energy Sciences, Office of Science, U.S. Department of Energy (Contract DE-FG02-13ER16428). R.M.C. also thanks the Robert A. Welch Foundation (Grant F-0032) for sustained support. Computing time was provided by the National Energy Research Scientific Computing Center and the Texas Advanced Computing Center at the University of Texas at Austin. We thank Mr. James A. Loussaert (UT-Austin) for performing the XPS analyses.

Supporting Information Available: Details about the DFT calculation and experimental procedures, nanoparticle characterization data, and a discussion of ORR activity are provided. This material is available free of charge *via* the Internet at http://pubs.acs.org.

REFERENCES AND NOTES

1. Adzic, R. R.; Zhang, J.; Sasaki, K.; Vukmirovic, M. B.; Shao, M.; Wang, J. X.; Nilekar, A. U.; Mavrikakis, M.; Valerio, J. A.; Uribe, F. Platinum Monolayer Fuel Cell Electrocatalysts. *Top. Catal.* **2007**, *46*, 249–262.
2. Adzic, R. R. Platinum Monolayer Electrocatalysts: Tunable Activity, Stability, and Self-Healing Properties. *Electrocatalysis* **2012**, *3*, 163–169.
3. Wang, C.; Chi, M.; Li, D.; Strmcnik, D.; Van Der Vliet, D.; Wang, G.; Komanicky, V.; Chang, K.; Paulikas, A. P.; Tripkovic, D.; *et al.* Design and Synthesis of Bimetallic Electrocatalyst with Multilayered Pt-Skin Surfaces. *J. Am. Chem. Soc.* **2011**, *133*, 14396–14403.
4. Zhang, L.; Henkelman, G. Tuning the Oxygen Reduction Activity of Pd Shell Nanoparticles with Random Alloy Cores. *J. Phys. Chem. C* **2012**, *116*, 20860–20865.
5. Sasaki, K.; Naohara, H.; Choi, Y.; Cai, Y.; Chen, W.-F.; Liu, P.; Adzic, R. R. Highly Stable Pt Monolayer on PdAu Nanoparticle Electrocatalysts for the Oxygen Reduction Reaction. *Nat. Commun.* **2012**, *3*, 1115.
6. Koenigsmann, C.; Sutter, E.; Adzic, R. R.; Wong, S. S. Size- and Composition-Dependent Enhancement of Electrocatalytic Oxygen Reduction Performance in Ultrathin Palladium–Gold ($Pd_{1-x}Au_x$) Nanowires. *J. Phys. Chem. C* **2012**, *116*, 15297–15306.
7. Carino, E. V.; Kim, H. Y.; Henkelman, G.; Crooks, R. M. Site-Selective Cu Deposition on Pt Dendrimer-Encapsulated Nanoparticles: Correlation of Theory and Experiment. *J. Am. Chem. Soc.* **2012**, *134*, 4153–4162.
8. Yancey, D. F.; Zhang, L.; Crooks, R. M.; Henkelman, G. Au@Pt Dendrimer Encapsulated Nanoparticles as Model Electrocatalysts for Comparison of Experiment and Theory. *Chem. Sci.* **2012**, *3*, 1033–1040.
9. Ye, H.; Crooks, R. M. Electrocatalytic O_2 Reduction at Glassy Carbon Electrodes Modified with Dendrimer-Encapsulated Pt Nanoparticles. *J. Am. Chem. Soc.* **2005**, *127*, 4930–4934.
10. Ye, H.; Crooks, R. M. Effect of Elemental Composition of PtPd Bimetallic Nanoparticles Containing an Average of 180 Atoms on the Kinetics of the Electrochemical Oxygen Reduction Reaction. *J. Am. Chem. Soc.* **2007**, *129*, 3627–3633.
11. Myers, V. S.; Weir, M. G.; Carino, E. V.; Yancey, D. F.; Pande, S.; Crooks, R. M. Dendrimer-Encapsulated Nanoparticles: New Synthetic and Characterization Methods and Catalytic Applications. *Chem. Sci.* **2011**, *2*, 1632–1646.
12. Sasaki, K.; Wang, J. X.; Naohara, H.; Marinkovic, N.; More, K.; Inada, H.; Adzic, R. R. Recent Advances in Platinum Monolayer Electrocatalysts for Oxygen Reduction Reaction: Scale-up Synthesis, Structure and Activity of Pt Shells on Pd Cores. *Electrochim. Acta* **2010**, *55*, 2645–2652.
13. Yancey, D. F.; Carino, E. V.; Crooks, R. M. Electrochemical Synthesis and Electrocatalytic Properties of Au@Pt Dendrimer-Encapsulated Nanoparticles. *J. Am. Chem. Soc.* **2010**, *132*, 10988–10989.
14. Carino, E. V.; Crooks, R. M. Characterization of Pt@Cu Core@Shell Dendrimer-Encapsulated Nanoparticles Synthesized by Cu Underpotential Deposition. *Langmuir* **2011**, *27*, 4227–4235.
15. Viswanathan, V.; Hansen, H. A.; Rossmeisl, J.; Nørskov, J. K. Universality in Oxygen Reduction Electrocatalysis on Metal Surfaces. *ACS Catal.* **2012**, *2*, 1654–1660.
16. Mukerjee, S.; Srinivasan, S. Enhanced Electrocatalysis of Oxygen Reduction on Platinum Alloys in Proton Exchange Membrane Fuel Cells. *J. Electroanal. Chem.* **1993**, *357*, 201–224.
17. Bligaard, T.; Nørskov, J. K.; Dahl, S.; Matthiesen, J.; Christensen, C. H.; Sehested, J. The Brønsted–Evans–Polanyi Relation and the Volcano Curve in Heterogeneous Catalysis. *J. Catal.* **2004**, *224*, 206–217.
18. Nørskov, J. K.; Rossmeisl, J.; Logadottir, A.; Lindqvist, L.; Kitchin, J. R.; Bligaard, T.; Jónsson, H. Origin of the Overpotential for Oxygen Reduction at a Fuel-Cell Cathode. *J. Phys. Chem. B* **2004**, *108*, 17886–17892.
19. Wang, L.-L.; Johnson, D. D. Predicted Trends of Core-shell Preferences for 132 Late Transition-Metal Binary-Alloy Nanoparticles. *J. Am. Chem. Soc.* **2009**, *131*, 14023–14029.
20. Greeley, J.; Mavrikakis, M. Near-Surface Alloys for Hydrogen Fuel Cell Applications. *Catal. Today* **2006**, *111*, 52–58.
21. Greeley, J.; Mavrikakis, M. Alloy Catalysts Designed from First Principles. *Nat. Mater.* **2004**, *3*, 810–815.
22. Yang, J.; Yang, J.; Ying, J. Y. Morphology and Lateral Strain Control of Pt Nanoparticles *via* Core–Shell Construction Using Alloy AgPd Core toward Oxygen Reduction Reaction. *ACS Nano* **2012**, *6*, 9373–9382.
23. Knecht, M. R.; Weir, M. G.; Frenkel, A. I.; Crooks, R. M. Structural Rearrangement of Bimetallic Alloy PdAu Nanoparticles within Dendrimer Templates to Yield Core/Shell Configurations. *Chem. Mater.* **2008**, *20*, 1019–1028.
24. Weir, M. G.; Knecht, M. R.; Frenkel, A. I.; Crooks, R. M. Structural Analysis of PdAu Dendrimer-Encapsulated Bimetallic Nanoparticles. *Langmuir* **2010**, *26*, 1137–1146.
25. Kresse, G. Dissociation and Sticking of H_2 on the Ni(111), (100), and (110) Substrate. *Phys. Rev. B* **2000**, *62*, 8295–8305.
26. Kresse, G.; Hafner, J. First-Principles Study of the Adsorption of Atomic H on Ni(111), (100) and (110). *Surf. Sci.* **2000**, *459*, 287–302.